Research Article

Possible Effect of Pyrogallol on Tongue Squamous Cell Carcinoma SCC-25 Cells

An In Vitro Study

Rahma G. Mostafa[1], Ehab S. Abd-ElHamid[2], Amr H. Mostafa El-Bolok[3], Enas A. ELdin[3] and Safaa M. Tohamy[1]

[1]Department of Oral Pathology, Faculty of Dentistry, Assuit University, Assuit, Egypt
[2]Department of Oral Pathology, Faculty of Dentistry, Ain Shams University, Cairo, Egypt
[3]Department of Oral Pathology, Faculty of Dentistry, Minia University, Minia, Egypt

Abstract

Background: Oral squamous cell carcinoma (OSCC) is one of the most prevalent oral cancers, despite rapid improvement in chemotherapy, radiotherapy, and targeted gene therapy used in conjunction with mainstay surgery, the OSCC prognosis remains low. Previous studies have demonstrated anti-proliferative activity of polyphenols in cancer cells, Pyrogallol (PG) one of natural polyphenols, with cytotoxicity and apoptogenic effects on neoplastic and transformed cells, but not in normal cells. **Objective:** This study aims to investigate the effect of PG on tongue squamous cell carcinoma SCC-25 cells and evaluate possible apoptotic pathways on SCC-25 cells. **Methods:** Cytotoxicity was measured by MTT assay. Mode of cell death was determined using Image morphometric analysis and Estimation of caspase-3 by Real Time PCR. **Results:** MTT results showed that SCC-25 cells were sensitive to PG with an IC_{50} value of 19.17 ug/ml. Image morphometric analysis showed a decrease in the mean values of Nuclear Area Factor (NAF) of SCC-25 cells treated with Different concentrations of PG when compared to control cells. In addition, PG induced apoptosis by simultaneous up-regulation of capase-3.**Conclusions:** Different concentrations of PG have a cytotoxic effect on SCC-25 cells. PG was also found to be an effective anti-carcinogenic agent with less toxicity.

Keywords: SCC-25 cell line, Pyrogallol, Nuclear Area Factor, RT-PCR, Apoptosis

Introduction

Oral squamous cell carcinoma (OSCC) is one of the most prevalent oral cancers, with a higher risk in individuals less than 40 years of age, especially in developing countries (Aghbali et al., 2013). 354,864 new cases of lip and oral cancer were reported in 2018 and 177,384 people died from these types of cancer (Bray et al., 2018). The risk factors proposed involve micronutrient deficiencies, chronic trauma, poor oral hygiene and some specific microorganisms such as viruses (Lauritano et al., 2016).

OSCC remains one of the most complex problems in head and neck oncology, and tends to be a disfiguring and lethal disease with a dismal 50% to 60% five-year disease specific survival rate, most frequently diagnosed at late stages (about 60% of patients present with advanced stage disease at initial diagnosis) (Nör & Gutkind, 2018).

Despite rapid improvement in chemotherapy, radiotherapy, and targeted gene therapy used in conjunction with mainstay surgery, the OSCC prognosis remains low. This is responsible for the highly aggressive and metastatic form of oral cancer (Agulnik, 2012). New therapeutic approaches have therefore been investigated and naturally acquired agents with known anti-carcinogenic effects are the most promising (Mileo et al., 2020).

Polyphenols are common phytochemicals in many plants (including plant seasonings), vegetables, fruits, seeds, oils, and alcoholic and non-alcoholic drinks contained in high concentrations (Pérez-Jiménez et al., 2010).

Polyphenols are known as compounds with one or more hydroxyl functional groups connected to at least one aromatic ring. Natural poly-

phenols refer to a broad group of secondary metabolites of plants ranging from small molecules to intensely polymerized compounds (Manach et al., 2004).Previous studies have shown anti-proliferative activity of polyphenols in cancer cells, while no cytotoxicity has been found in non-cancer cells within the same treatment concentration range (Thangapazham et al., 2007).

Pyrogallol (PG) is a simple phenol that comprises three hydroxyl groups in the ortho- and metaposition respectively, of a benzene ring. Humans are exposed to PG by ingestion of tea and coffee (Muller et al., 2006), but also by decomposition of gallic acid in colon (Yasuda et al., 2000). PG itself has been shown to enhance O2•-mediated death / apoptosis of several types of cells, including human pulmonary adenocarcinoma Calu-6 cells (Han et al., 2009), As4.1 juxtaglomerular cells (Park et al., 2007), gastric cancer SNU-484 cells (Park et al., 2008), human histiocytic lymphoma U937 cells (Saeki et al., 2000) and endothelial cells (Han and Park, 2010). In addition, polyphenols containing the PG ring in their structures have been shown to cause apoptosis in human chronic myelogenous leukemia cell line K562 and human embryonic kidney HEK 293T cells (Mitsuhashi et al., 2008). PG also has cytotoxicity and apoptogenic effects on the neoplastic and transformed cells, but not in normal cells (Yang et al., 2009).

The purpose of this study is to investigate the possible apoptotic and cytotoxic effects of PG on SCC-25 cells evaluate the cytological changes that might occur in PG treated cells compared to untreated control cells, analyze the nuclear morphometric changes of PG treated cells and evaluation of caspase-3 gene expression.

Material and methods

I. Material

Cell line

Human tongue squamous carcinoma cell line (SCC-25), was collected from the cell culture department- VACSERA-EGYPT. SCC-25 cells were imported from the "American type Culture Collection (ATCC)" in the form of frozen vial with the reference number "CRL-1628".

Reagents

- **Drug**

PG (Sigma Aldrich-USA), with a molecular formula of $C_6 H_3 (OH)_3$ and a molecular weight of 126.11 g/mol, was the cytotoxic drug used in this research.

- **Cell Culture Medium**

1. Growth medium

Minimum essential medium modified with Hank's salts (MEM-H) supplemented with 10% foetal bovine serum (FBS), 2mM glutamine and sodium bicarbonate (Invitrogen, USA).

2. Foetal bovine serum (FBS)

FBS obtained from GIBO COBRAL® limited, Scotland as a sterile serum in 500 ml bottles (stored at -20°C until used).

II. Methods

Cytotoxicity assay

Methyl Thiazol Tetrazolium (MTT) assay uses yellow tetrazolium salt (3-[4,5-dimethylthiazol-2-yl]-2,5-diphenyltetrazolium bromide) which is water-soluble salt and is reduced to an insoluble purple MTT-formazan complex by cleavage of the tetrazolium ring by Lactate Dehydrogenase (LDH) inside the mitochondria. This reduction occurs only when mitochondrial reductase enzymes are active, so the conversion can be directly linked to the number of viable (living) cells. The MTT viability test measures the rate of cell proliferation and, conversely, cell viability is decreased when metabolic events leading to apoptosis or necrosis occur. The resulting intracellular purple formzan crystals can be solubilized and quantified by spectrophotometric means. (Bahuguna et al., 2017). Results were determined as the means of independent experiments. The viability percentage was calculated as following:

Viability percentage = X Absorbance of test dilution x 100X Absorbance mean of control

The data collected were analyzed using Master Plex Reader Fit program to determine the IC_{50}, the half maximal inhibitory concentration of PG.

Microscopic examination

After preparation of the slide, Hematoxylin and Eosin Staining was applied by following steps:

• The fixed slides were rehydrated at low alcohol concentrations (100%, 90%, 75% then

50%) and then washed in distilled water for 5 min.

• The slides were submerged n filtered hematoxylin stain for 3 min and then washed with distilled water twice.

• The slides were soaked in filtered eosin stain for 5 seconds and then washed with distilled water.

• Dried slides were soaked in xylene, mounted with Canada balsam then coverslips were placed and left to dry.

Assessment of Hematoxylin and Eosin stained SCC-25 cells

a) Photomicrography and cytological evaluation:

Thirty microscopic fields of each group were photomicrographed at power of 1000X (Oil immersion). This was achieved using a digital video camera (Canon, Japan) which was mounted on a light microscope (Olympus BX60, Japan). Then, images were transferred to the computer system for analysis. The selection of field was based on the existence of the highest number of apoptotic cells. The photomicrographs were assessed for the presence of morphological criteria of apoptosis.

b) Nuclear Morphometric Analysis:

The photomicrograph fields were analyzed using image analysis software (Image J, 1.27z, NIH, USA). Images have been checked for brightness and contrast automatically. Corrected images have been converted into 8-bit grayscale type. The phase color coding was done automatically for the desired region. For selecting the nuclei of SCC-25 cells, the color threshold was adjusted. In order to standardize the method for all analyzed images, attempts were made to reduce the operator guided in favor of the automatic thresholding throughout this step. The surface area and circularity of the nuclei were automatically measured. Nuclear area factor has been determined using the following formula (DeCoster, 2007):

Nuclear area factor = Circularity x Object area

The data were then tabulated in Microsoft Excel sheet (Microsoft Office 2010®).

c) Statistical Analysis

The mean values of the nuclear area factor (NAF) of PG for control results were statistically assessed using the Social Science Statistical Package (SPSS 16.0) window software. The statistical methods carried out included a variance analysis (ANOVA) to compare the mean PG. The findings were assumed to be meaningful if the value of P was <0.05. A multiple comparison test (Turkey HSD) was conducted post hoc. Using SPSS software, graphs reflecting error bars of mean ± standard error were carried out.

Estimation of caspase-3 by Real Time PCR

Complete RNA was extracted from control and treated SCC-25 using RNeasy micro kit Cat.no 74004 according to the manufacturer`s protocol. The concentration and integrity of RNA were measured spectrophotometrically at 260/280 nm ratio. First-strand cDNA was synthesized with 1µ of total RNA using a Quantitect Reverse Transcription Kit [Qiagen, Germany] in conjunction with the manufacturer`s instructions. These samples were subsequently frozen at a temperature of -80ºC until they were used to determine expression level of caspase-3 gene using real-time PCR. Quantitative real-time PCR was performed on a Rotor-Gene Q cycler [Qiagen, Germany] using the QuantiTect SYPR Green PCR kits [Qiagen, Germany] and forward and reverse primer for gene.

Results

Cytotoxicity assay

SCC-25 cells were treated with different concentration (0.39, 1.56, 6.25, 25, 100 ug/ml) of PG for 24 h. The percentage of the surviving PG treated cells compared with the untreated cells is presented in Fig. 1a. After 24h from treatment with increasing doses of PG (0.39 ug - 100 ug), cell growth was inhibited in a dose dependent manner, where 19.17 ug/ml of PG were able separately to inhibit the cell growth to 50% (Fig. 1b).

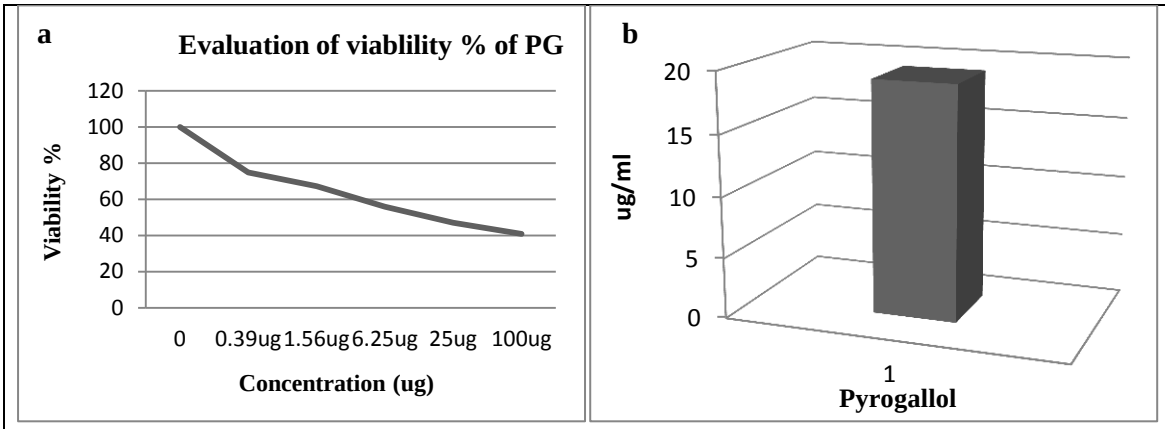

Figure (1): (a) Evaluation of viability percentage of SCC-25 post treatment with different concentrations of PG for 24 hours; **(b)** Evaluation of IC_{50} post SCC-25 cell treatment with PG.

Microscopic examination

I. Cytological evaluation

1. Control cells

Most of SCC-25 cells showed almost rounded, hyperchromatic nuclei and the cellular outline was almost regular without evidence of any folding. Only a few cells among control cells showed criteria of apoptosis mainly confined to nuclear shrinkage and chromatin condensation (Fig. 2A).

2. PG treated SCC-25 cells

24 hours post treatment with pre IC_{50}, IC_{50} and post IC_{50} concentrations of PG for 24 hours showed apoptotic morphological changes, necrotic features and secondary necrosis. Many cells showed morphological alterations that matched with morphological criteria of apoptosis. These criteria included nuclear shrinkage, nuclear fragmentation, membrane blebbing, and apoptotic bodies. On the other hand, with IC_{50} concentration of PG, the presence of apoptotic morphological changes was more obviously seen (Fig. 2)

In addition to these apoptotic criteria, fewer cells showed morphological alterations that matched with morphological criteria of necrosis especially with post IC_{50} concentration of PG.

These criteria included clumping of heterochromatin admixed with euchromatin, nuclear and cellular swelling and rupture in the cell membrane. Presence of cells observing both necrotic and apoptotic features such as nuclear fragmentation and cytoplasmic swelling in the same cell (secondary necrosis) was also seen (Fig. 2).

Fig. (2): (A) photomicrograph of control SCC-25 cell 24 hours showing pleomorphism, hyperchromatism and cell with nuclear shrinkage (blue arrow); **(B)** SCC-25 cell 24 hours post treatment with pre IC_{50} concentration of PG showing nuclear shrinkage (blue arrow), membrane blebbing (red arrow), apoptotic body (green arrow), nuclear fragmentation (orange arrow), swollen necrotic cell (violet arrow) and cell debris (yellow arrows); **(C)** SCC-25 cell 24 hours post treatment with IC_{50} concentration of PG showing nuclear shrinkage (blue arrow), membrane blebbing (red arrows), apoptotic body (green arrows), peripheral chromatin condensation (black arrow), nuclear fragmentation (orange arrow), irregular nuclear and cellular outlines (gray arrow), patchy chromatin (violet arrow), necrotic body (brown arrow) and cell debris (yellow arrow); **(D)** SCC-25 cell 24 hours post treatment with post IC_{50} concentration of PG showing nuclear shrinkage (blue arrow), apoptotic bodies (green arrows), peripheral chromatin condensation (black arrow), nuclear fragmentation (orange arrow), necrotic body (brown arrow), secondary necrotic cell (red arrows), swollen necrotic cell with clumping of heterochromatin admixed with euchromatin (violet arrow) and cell debris (yellow arrows) (H & E x 1000 oil).

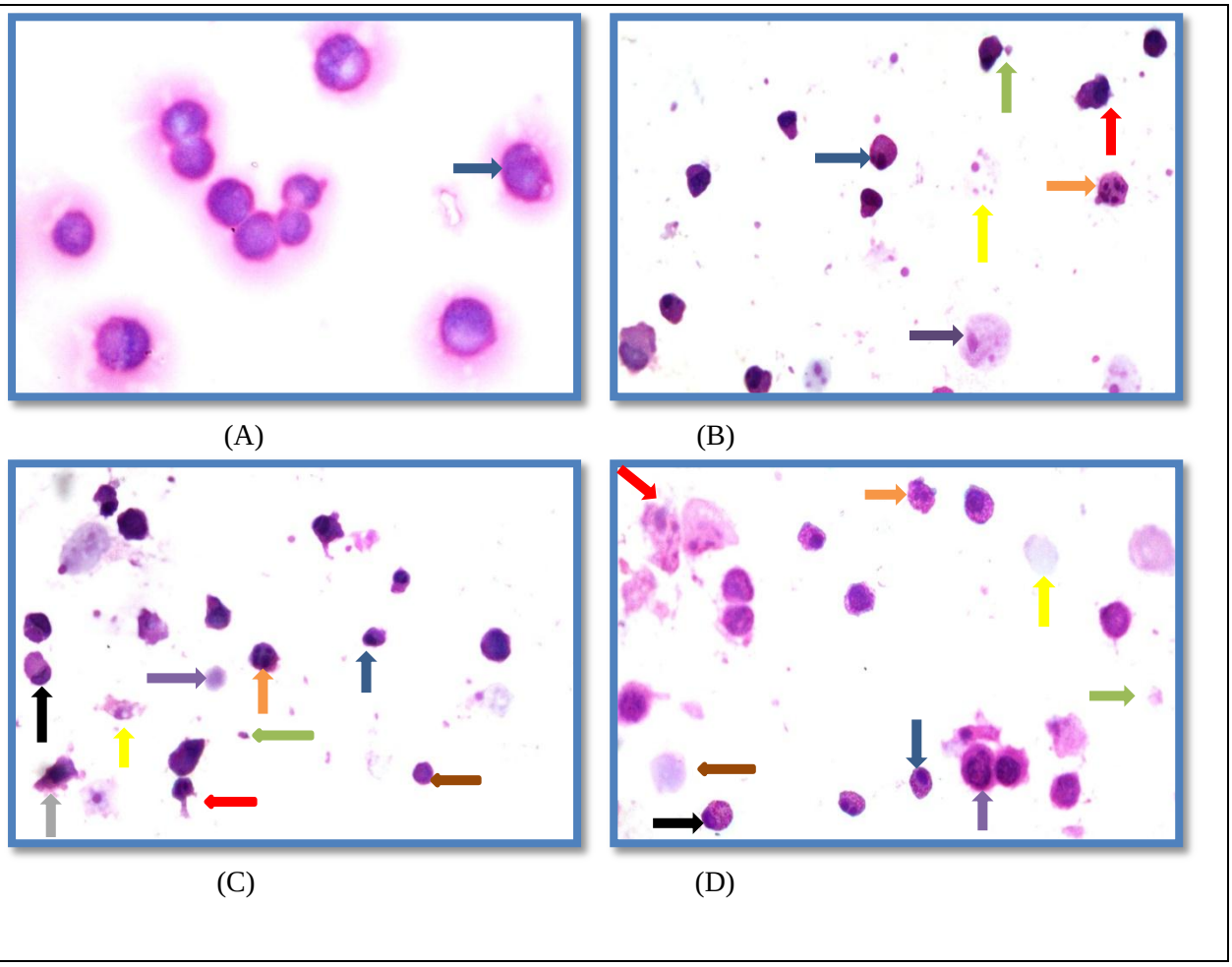

II. Morphometric analysis

Nuclear area factor (NAF)

The mean NAF values for SCC-25 cells treated with different concentrations of PG are shown in table (1). The data recorded showed a decrease in the mean values of NAF of SCC-25 cells treated with different concentrations of PG when compared to control cells (Figure 3).

Table (1): The mean values of NAF of control and SCC-25 cells treated with different concentrations of PG after 24 hours (descriptive statistics).

Group	Control cells	Pre IC_{50}	IC_{50}	Post IC_{50}
NAF	9579.82	2330.86	1233.25	1024.87

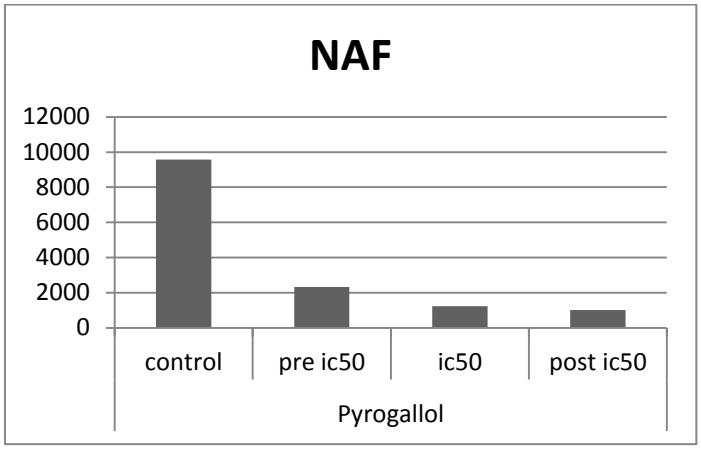

Figure (3): A histogram displaying the mean values of NAF of control and SCC-25 cells treated with different concentrations of PG.

Effect of Pyrogallol concentrations on NAF

Table (2) demonstrates the mean NAF values ± standard control deviation and 24-hour SCC-25 treated cells with different PG concentrations. The ANOVA test showed a statistically high difference between the mean NAF values of the SCC-25 cells treated with different PG concentrations and the control cells (P value < 0.000) (Table 3).

Post Hoc Multiple Comparison Test (Bonferroni) showed a statistically insignificant difference between the mean NAF values of the SCC-25 cells treated with different PG concentrations. However there was a statistically significant difference between the mean NAF values of the SCC-25 cells treated with different PG concentrations relative to the mean NAF values of the control cells after 24 hours (Table 4).

Table (2): The mean values of NAF ± stranded deviation of control as well as SCC-25 cells treated by different concentrations of PG after 24 hours (descriptive statistics).

	Mean	Standard Deviation	Standard Error of Mean	Minimum	Maximum	95.0% Lower CL for Mean	95.0% Upper CL for Mean
control	9579.82	2409.02	761.80	5665.76	13401.61	7856.51	11303.13
Pre IC_{50}	2330.86	909.65	287.66	1493.41	4067.04	1680.13	2981.58
IC_{50}	1233.25	819.55	259.16	297.29	3034.73	646.98	1819.52
Post IC_{50}	1024.87	798.74	252.59	283.57	2692.80	453.49	1596.26

Table (3): The mean values of NAF of different PG concentrations and control cells 24 hours post treatment (ANOVA test).

	Sum of Squares	df	Mean Square	F	Sig.
Between Groups	495883385.677	3	165294461.892	83.267	0.000
Within Groups	71464485.035	36	1985124.584		
Total	567347870.712	39			

Table (4): Comparison of mean difference NAF ± standard error for different PG concentrations and control cells 24 hours post treatment (Post Hoc multiple comparisons test (Bonferroni))

(I)group	(J) group		Mean Difference (I-J)	Std. Error	Sig.	95% Confidence Interval	
						Lower Bound	Upper Bound
	control	pre ic50	7248.96080*	630.09913	0.000	5489.7417	9008.1799
		ic50	8346.56450*	630.09913	0.000	6587.3454	10105.7836
		post ic50	8554.94240*	630.09913	0.000	6795.7233	10314.1615
	pre ic50	control	-7248.96080-*	630.09913	0.000	-9008.1799	-5489.7417
		ic50	1097.60370	630.09913	0.540	-661.6154	2856.8228
		post ic50	1305.98160	630.09913	0.273	-453.2375	3065.2007
	ic50	control	-8346.56450-*	630.09913	0.000	-10105.7836	-6587.3454
		pre ic50	-1097.60370	630.09913	0.540	-2856.8228	661.6154
		post ic50	208.37790	630.09913	1.000	-1550.8412	1967.5970
	post ic50	control	-8554.94240-*	630.09913	0.000	-10314.1615	-6795.7233
		pre ic50	-1305.98160	630.09913	0.273	-3065.2007	453.2375
		ic50	-208.37790	630.09913	1.000	-1967.5970	1550.8412

PCR (Caspase-3 fold change)

Treatment of SCC-25 cells with various concentrations of PG cause significant upregulation of Caspase-3 gene fold change compared to control cells (Table 5) (Fig. 4).

Table (5): Caspase-3 gene fold change using RT-PCR in different concentrations of PG

Sample data		Results fold change	
SCC-treated cell with PG	Pre IC50	5.27	
	IC50	8.18	
	Post IC50	8.71	
Control cells	----	1	

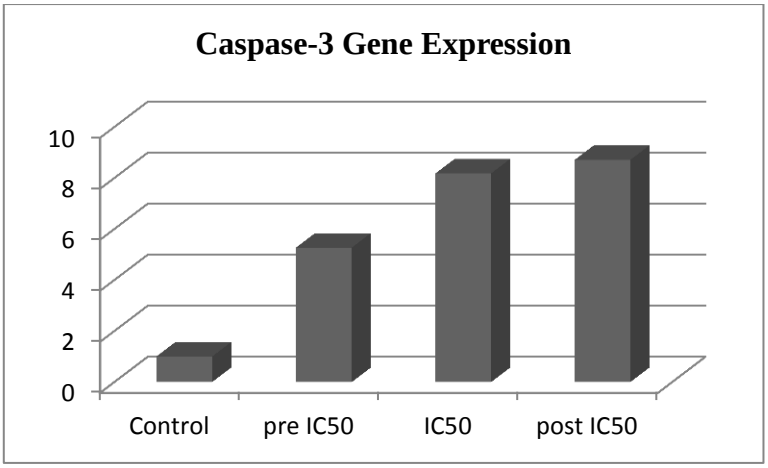

Figure (4): Evaluation of the expression of the caspase-3 gene in different concentrations of SCC-25 cells treated with PG relative to control cells.

Discussion

After 24 h of treatment with PG, SCC-25 showed dose dependent decline in cell survival. Interestingly SCC-25 cells are sensitive to PG with an IC_{50} value of 19.17 ug / ml. To our knowledge, in English literature, no research was conducted to investigate the effect of PG in relation to inhibition of OSCC cancer cells as this is the first time that PG has been prepared, and in turn, the current results are supported by researches using different cancer cells.

Consistent with the present results, the findings revealed by Han and Park 2010 indicate that PG inhibited cell growth and induced apoptosis of As4.1, which was associated with the loss of mitochondrial membrane potential (MMP). Furthermore, the current findings are in accordance with Revathi et al., 2018, which showed that PG induces dose-dependent cytotoxicity in HT-29 colon cancer cells and that cytotoxicity is attributable to its phenolic structure with three ring ortho-position hydroxyl groups. It is well known that dihydroxylated phenolic compounds show less cytotoxicity than orthotrihydroxylated phenolic compounds in breast cancer (MCF-7 cells) (Fernandes et al., 2010).

In addition, the current findings are consistent with Ahn et al., 2019, which showed that PG significantly increased cytotoxicity and decreased the number of colonies in Hep3B and Huh7 hepatocellular carcinoma cells (HCCs), suggesting the cytotoxic and anti-proliferative effects of PG.

In the present study, PG SCC-25 cells were cytologically evaluated to compare cancer cells before and after PG administration in order to predict the effect of the drug on apoptosis induction. The benefit of this approach was that it was simple and convenient with low costs (Shtilbans & Burstein, 2010). SCC-25 cells treated with 24-hour pre-IC_{50}, IC_{50} and post-IC_{50} PG concentrations demonstrated apoptotic morphological changes, necrotic features and secondary necrosis. Necrotic criteria and secondary necrosis were more dominant in post-IC_{50} concentrations than in pre-IC_{50} and IC_{50} concentrations of PG. While apoptotic morphological changes such as nuclear shrinkage, nuclear fragmentation, nuclear membrane irregularities, peripheral chromatin condensation, cell membrane blebbing and apoptotic bodies have become more apparent at IC_{50} concentration of PG.

The current PG findings are consistent with Saeki et al., 2000, which showed that the PG induction of apoptosis was indicated by a PG-type structure in the B-ring of catechins. DNA fragmentation activity in histiocytic lymphoma U937 cells was shown in a concentration-dependent manner after treatment with catechins containing a PG-type structure in the β-ring. While catechins without a PG-type structure in any position did not show

apoptosis-inducing activity. In addition, human cervical adenocarcinoma HeLa cells treated with 60 mM of PG at 72 h showed typical morphological features of apoptosis cells as condensed nucleus and separated apoptotic bodies (Kim et al., 2008).

Furthermore, current findings are consistent with Revathi et al., 2018, which showed that 24hours of PG therapy induces significant apoptotic morphology, such as cell shrinkage, nuclear condensation and fragmentation, and the formation of apoptotic bodies in HT-29 colon cancer cells.

There are a variety of biochemical and image-based apoptosis essays that differ widely in complexity, specificity and cost. It has previously been shown that the nuclear area factor (NAF) can be an early and sensitive predictor of cell morphological changes occurring during apoptosis because it is dependent on two essential morphological parameters of apoptosis (DeCoster, 2007). The NAF was measured (surface area x circularity) using Image J, 1.27z (Afify et al., 2012).

The NAF of SCC-25 cells treated by different concentrations of PG for 24 hours were compared as well as with NAF of control untreated cells. Where decreasing in NAF means that there were apoptotic changes.

The ANOVA test showed that the mean NAF values of SCC-25 cells treated with different concentrations of PG decreased relative to control untreated cells. These findings have confirmed the appearance of apoptotic changes.

This decrease is encouraged in the cytological inspection, which showed an increase in apoptotic morphological changes at different concentrations of PG. In addition, the lowest decrease in mean NAF value occurred at post-IC_{50} PG concentration relative to control untreated cells. Thus at that concentration, apoptosis plays a key role in cell death.

A common part of various apoptotic signaling pathways is Caspase-3, which is the convergence point of the apoptotic signaling pathway. Once caspase-3 was activated, apoptotic pathways were initiated (Yin et al., 2016). Caspase-3 is a caspase executioner whose activation will systematically dismantle cells by cleaving main proteins such as poly (ADP-ribose) polymerase (PARP) (Bruges et al., 2018). The activation pathways for Caspase-3 were established as both mitochondrial cytochrome c release and caspase-9 function dependent and non-dependent (Yang et al., 2007).

In the current study it was detected that, the expression of caspase-3 increased in SCC-25 treated cells with different concentrations of PG when compared to control non treated cells.

As regards the gene expression profile, caspase-3 activation is critical for the process of PG-induced cell death (Han et al., 2009). The current findings are in accordance with Park, which stated in 2016 that PG had apparently increased caspase-3 activity and reduced the precursor form of this caspase. Furthermore, the current findings agree with Bruges et al., 2018, which showed that PG induces additional mitochondrial apoptotic events downstream, including the activation of apoptosis executioner caspase-3 on the plasma membrane platelet's outer leaflet. In addition, PG induced apoptosis in HT-29 colon cancer cells by down regulating the apoptosis activator Bcl-2 with high expression of cytochrome c which leads to establishment of apoptosome in the cytosol and initiation of caspase signaling cascade. This may be due to PG's free radical scavenging capacity (Revathi et al., 2018).

Conclusions

It can be inferred on the basis of the results of the current study that: PG has a cytotoxic effect on the cells of SCC-25. In addition, the NAF estimate is a sensitive predictor of early apoptotic effect of anti-cancer treatment. Moreover, PG induced apoptosis through upregulation of caspase-3.

References

1. Aghbali, A., Hosseini, S. V., Delazar, A., Gharavi, N. K., Shahneh, F. Z., Orangi, M. ... & Baradaran, B. (2013). Induction of apoptosis by grape seed extract (Vitis vinifera) in oral squamous cell carcinoma. Bosnian journal of basic medical sciences, 13(3), 186.
2. Bray, F., Ferlay, J., Soerjomataram, I., Siegel, R. L., Torre, L. A., & Jemal, A.

(2018). Global cancer statistics 2018: GLOBOCAN estimates of incidence and mortality worldwide for 36 cancers in 185 countries. CA: a cancer journal for clinicians, 68(6), 394-424.

3. Lauritano, D., Lucchese, A., Contaldo, M., Serpico, R., Lo Muzio, L., Biolcati, F., & Carinci, F. (2016). Oral squamous cell carcinoma: diagnostic markers and prognostic indicators.
4. Agulnik, M. (2012). New approaches to EGFR inhibition for locally advanced or metastatic squamous cell carcinoma of the head and neck (SCCHN). Medical Oncology, 29(4), 2481-2491.
5. Nör, J. E., & Gutkind, J. S. (2018). Head and neck cancer in the new era of precision medicine. 601-602.
6. Mileo, A. M., Di Venere, D., Mardente, S., & Miccadei, S. (2020). Artichoke Polyphenols Sensitize Human Breast Cancer Cells to Chemotherapeutic Drugs via a ROS-Mediated Downregulation of Flap Endonuclease 1. Oxidative Medicine and Cellular Longevity, 2020.
7. Pérez-Jiménez, J., Neveu, V., Vos, F., & Scalbert, A. (2010). Identification of the 100 richest dietary sources of polyphenols: an application of the Phenol-Explorer database. European journal of clinical nutrition, 64 Suppl 3, S112–S120.
8. Manach, C., Scalbert, A., Morand, C., Rémésy, C., & Jiménez, L. (2004). Polyphenols: food sources and bioavailability. The American journal of clinical nutrition, 79(5), 727-747.
9. Thangapazham, R. L., Singh, A. K., Sharma, A., Warren, J., Gaddipati, J. P., & Maheshwari, R. K. (2007). Green tea polyphenols and its constituent epigallocatechin gallate inhibit proliferation of human breast cancer cells in vitro and in vivo. Cancer letters, 245(1-2), 232-241.
10. Müller, C., Lang, R., & Hofmann, T. (2006). Quantitative precursor studies on di-and trihydroxybenzene formation during coffee roasting using “in bean” model experiments and stable isotope dilution analysis. Journal of agricultural and food chemistry, 54(26), 10086-10091.
11. Yasuda, T., Inaba, A., Ohmori, M., Endo, T., Kubo, S., & Ohsawa, K. (2000). Urinary metabolites of gallic acid in rats and their radical-scavenging effects on 1, 1-diphenyl-2-picrylhydrazyl radical. Journal of Natural Products, 63(10), 1444-1446.
12. Han, Y. H., Kim, S. Z., Kim, S. H., Park, W. H. (2009) Pyrogallol inhibits the growth of lung cancer Calu-6 cells via caspase-dependent apoptosis. Chem. Biol. Interact. 177, 107-114.
13. Park, W. H., Han, Y. H., Kim, S. H., Kim, S. Z. (2007) Pyrogallol, ROS generator inhibits As4.1 juxtaglomerular cells via cell cycle arrest of G2 phase and apoptosis. Toxicology 235, 130-139.
14. Park, W. H., Park, M. N., Han, Y. H., Kim, and S.W. (2008) Pyrogallol inhibits the growth of gastric cancer SNU-484 cells via induction of apoptosis. Int. J. Mol. Med. 22, 263-268.
15. Saeki, K., Hayakawa, S., Isemura, M., Miyase, T. (2000) Im-portance of a pyrogallol-type structure in catechin compounds for apoptosis-inducing activity. Phytochemistry 53, 391-394.
16. Han, Y. H., Park, W. H. (2010) Pyrogallol-induced calf pulmonary arterial endothelial cell death via caspase-dependent apoptosis and GSH depletion. Food Chem. Toxicol. 48, 558-563.
17. Mitsuhashi, S., Saito, A., Nakajima, N., Shima, H., Ubukata, M. (2008) Pyrogallol structure in polyphenols is involved in apoptosis-induction on HEK293T and K562 cells. Molecules 13, 2998-3006.
18. Yang, C. J., Wang, C. S., Hung, J. Y., Huang, H. W., Chia, Y. C., Wang, P. H. ... & Huang, M. S. (2009). Pyrogallol induces G2-M arrest in human lung cancer cells and inhibits tumor growth in an animal model. Lung Cancer, 66(2), 162-168.
19. Bahuguna, A., Khan, I., Bajpai, V. K., & Kang, S. C. (2017). MTT assay to evaluate the cytotoxic potential of a drug. Bangladesh Journal of Pharmacology, 12(2), Online-Apr.
20. DeCoster, M. A. (2007). The nuclear area factor (NAF): a measure for cell apoptosis using microscopy and image analysis. Modern research and educational topics in microscopy, 1, 378-84.
21. Revathi, S., Hakkim, F. L., Kumar, N. R., Bakshi, H. A., Rashan, L., Al-Buloshi, M. ... & Nagarajan, K. (2018). Induction of HT-29 colon cancer cells apoptosis by Pyrogallol with growth inhibiting efficacy

against drug-resistant Helicobacter pylori. Anti-Cancer Agents in Medicinal Chemistry (Formerly Current Medicinal Chemistry-Anti-Cancer Agents), 18(13), 1875-1884.

22. Fernandes, I., Faria, A., Azevedo, J., Soares, S., Calhau, C., De Freitas, V., & Mateus, N. (2010). Influence of anthocyanins, derivative pigments and other catechol and pyrogallol-type phenolics on breast cancer cell proliferation. Journal of agricultural and food chemistry, 58(6), 3785-3792.
23. Ahn, H., Im, E., Lee, D. Y., Lee, H. J., Jung, J. H., & Kim, S. H. (2019). Antitumor Effect of Pyrogallol via miR-134 Mediated S Phase Arrest and Inhibition of PI3K/AKT/Skp2/cMyc signaling in Hepatocellular Carcinoma. International journal of molecular sciences,20(16), 3985.
24. Shtilbans, V., Wu, M., & Burstein, D. E. (2010). Evaluation of apoptosis in cytologic specimens. Diagnostic Cytopathology, 38(9), 685-697.
25. Kim, S. W., Han, Y. W., Lee, S. T., Jeong, H. J., Kim, S. H., Kim, I. H., ... & Park, W. H. (2008). A superoxide anion generator, pyrogallol, inhibits the growth of HeLa cells via cell cycle arrest and apoptosis. Molecular Carcinogenesis: Published in cooperation with the University of Texas MD Anderson Cancer Center, 47(2),114-125.
26. Afifi, N. S., Abdel-Hamid, E. S., Baghdadi, H. M., & Mohamed, A. F. (2012). Nuclear Area Factor as a Novel Estimate for Apoptosis in Oral Squamous Cell Carcinoma-Treated Cell Line: A Comparative in-vitro Study with DNA Fragmentation Assay. Journal of Clinical & Experimental Pathology, 2(2), 1-5.
27. Yin, C., Huang, G. F., Sun, X. C., Guo, Z., & Zhang, J. H. (2016). Tozasertib attenuates neuronal apoptosis via DLK/JIP3/MA2K7/JNK pathway in early brain injury after SAH in rats. Neuropharmacology, 108, 316-323.
28. Bruges, G., Venturini, W., Crespo, G., & Zambrano, M. L. (2018). Pyrogallol induces apoptosis in human platelets. Folia biologica, 64(1), 23-30.
29. Yang, S., Zhou, Q., & Yang, X. (2007). Caspase-3 status is a determinant of the differential responses to genistein between MDA-MB-231 and MCF-7 breast cancer cells. Biochimica ET Biophysica Acta (BBA)-Molecular Cell Research, 1773(6), 903-911.
30. Park WH. (2016): Pyrogallol induces the death of human pulmonary fibroblast cells through ROS increase and GSH depletion. Int. J. of Oncology (49): 785-792.